Optik 156 (2018) 8–12

Contents lists available at ScienceDirect

Optik

journal homepage: www.elsevier.de/ijleo

Original research article

Synthesis and VUV photoluminescence of $Y_2O_3:Eu^{3+}$ by doping different ions

Lei Zhao[a,*], Deyin Wang[b], Dandan Meng[a], Wenbo Chen[c,*]

[a] College of Physics and Optoelectronic Technology, Baoji University of Arts and Sciences, Baoji 721016, PR China
[b] Department of Materials Science, School of Physical Science and Technology, Lanzhou University, Lanzhou 730000, PR China
[c] Engineering Research Center of New Energy Storage Devices and Applications, Chongqing University of Arts and Sciences, Chongqing, 402160, PR China

ARTICLE INFO

Article history:
Received 11 August 2017
Accepted 25 October 2017

Keywords:
Optical material
Oxide
Luminescence

ABSTRACT

Eu^{3+}-activated Y_2O_3 phosphors doped with M (M = Gd^{3+}, La^{3+}, Zn^{2+}, Li^+) were synthesized via a low temperature hydrothermal method with subsequent heat treatment. The photoluminescent properties of Eu^{3+}-activated Y_2O_3 with different M ions under 147 nm excitation were examined. The excitation spectra of all samples consisted of two bands with maxima at about 207 nm and 239 nm. The former band was ascribed to the band edge of Y_2O_3, and the latter band was assigned to the charge transfer transition between Eu^{3+} and O^{2-}. At the same doping concentration, Gd^{3+} or Li^+ doping had a positive effect on the luminescence of $Y_2O_3:Eu^{3+}$, while La^{3+} or Zn^{2+} doping had a negative effect. The mechanism and role of different M ions were discussed.

1. Introduction

Yttrium oxide has numerous applications in various fields, such as laser materials [1,2], catalyst support or even catalysts [3,4], advanced ceramics [5,6] and transparent matrices for phosphor materials when doping with rare earth metals [7–9]. Particularly, Eu^{3+} activated Y_2O_3 is one of the most frequently used commercial lighting and cathode-ray phosphors [10–12]. Moreover, it is a promising phosphor developed for field emission displays (FED) [13,14] and plasma display panels (PDP) [15]. However, although $Y_2O_3:Eu^{3+}$ has a better color purity than $(Y,Gd)BO_3:Eu^{3+}$ which is an efficient red phosphor used in PDP [16], its luminescence efficiency is much lower than that of $(Y,Gd)BO_3:Eu^{3+}$ under vacuum ultraviolet (VUV) excitation. In the present paper, we synthesized $Y_2O_3:Eu^{3+}$ by a mild hydrothermal method with subsequent heat treatment, and added different M ions (M = Gd^{3+}, La^{3+}, Zn^{2+}, Li^+) to $Y_2O_3:Eu^{3+}$ in anticipation of improving its VUV luminescence efficiency. Our choice of M as doping ions is mainly motivated by the following facts: Firstly, Gd^{3+} has been shown to be a good sensitizer, which can greatly improve the luminescent efficiency of phosphors in the VUV region [17,18]. Secondly, $[ZnO_4]^{2-}$ has an absorption around 157 nm in $Zn_2SiO_4:Mn^{2+}$ [19], so adding Zn^{2+} may increase the VUV luminescence efficiency of $Y_2O_3:Eu^{3+}$. Thirdly, the incorporation of La^{3+} to phosphors can improve the luminescence to a certain extent [20]. Finally, the Li^+ co-activators frequently play an important role in enhancing luminescent efficiency of phosphors [21].

* Corresponding authors.
E-mail addresses: zhaoleibjwl@163.com (L. Zhao), qschenbo@sina.com (W. Chen).

https://doi.org/10.1016/j.ijleo.2017.10.140
0030-4026/

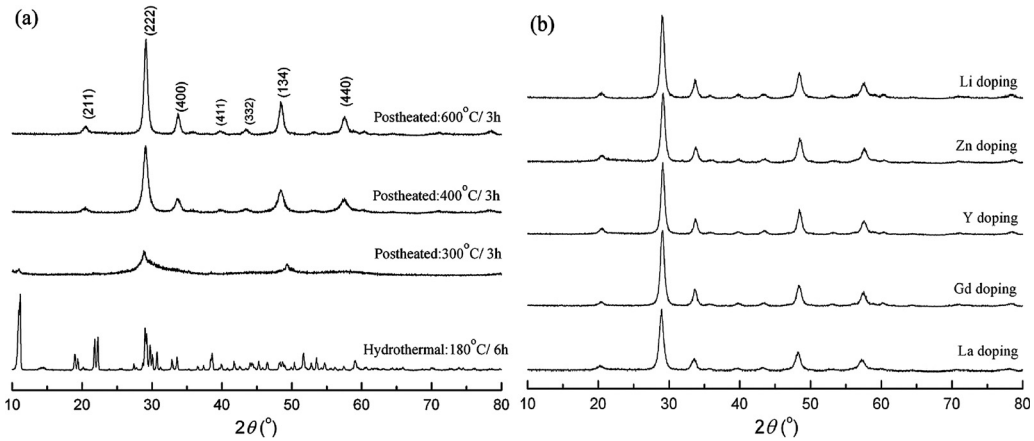

Fig. 1. XRD patterns of $Y_{1.95}O_3$:0.05Eu^{3+} prepared using hydrothermal method before and after post-calcinations (a) and $Y_{1.85}M_{0.1}O_3$:0.05Eu^{3+} (M = Gd, Y, La, Zn, Li) prepared using hydrothermal method after post-heated at 600 °C for 3 h (b).

2. Experimental

$Y_{1.85}M_{0.1}O_3$:0.05Eu^{3+} (M = Gd, Y, La, Zn, Li) were prepared via a low temperature hydrothermal method with subsequent heat treatment. The starting materials were Y_2O_3 (99.99%), Gd_2O_3 (99.99%), La_2O_3 (99.99%), ZnO (A.R.) and Li_2CO_3 (A.R.). To prepare $Y_{1.85}M_{0.1}O_3$:0.05Eu^{3+}, corresponding raw materials were dissolved in nitric acid, and then the pH of the solution was adjusted to about 9 by adding $NH_3{\cdot}H_2O$ solution. The resulting precipitates were then transferred into a 30-ml autoclave, which was filled with distilled water up to 80% of the total volume, sealed, and then heated at 180 °C for about 6 h. After natural cooling, the precipitates were filtrated, washed with distilled water several times and dried in an oven (90 °C) to get the white precursor. The as-synthesized precursors were then sintered at different temperatures for 3 h in air to yield the final products.

The X-ray diffraction (XRD) patterns were recorded by using a Rigaku D/max-2000 Diffractometer with Cu Kα radiation. Particle sizes and shapes were determined by a transmission electron microscope (TEM) (200CX, JEOL, Japan) operated at 160 kV. The differential thermal analysis (DTA) and thermogravimetric (TG) analysis was carried out with a Perkin-Elmer Thermal Analyzer (Diamond, USA) at a rate of 10 °C/min between 40 ~ 800 °C, to analyze the decomposition reaction and phase transformation of the precursor. The VUV excitation and emission spectra were measured by a VM-504-type vacuum monochromator with a deuterium lamp as the lighting source. The excitation spectra were corrected with sodium salicylate.

3. Results and discussion

For a reference, Fig. 1(a) shows the XRD patterns of $Y_{1.95}O_3$:0.05Eu^{3+} prepared using the hydrothermal method before and after post-calcinations. It can be seen from Fig. 1(a), before post-thermal treatment, that the hydrothermal product can be readily indexed to that of the monoclinic phase of $Y_4O(OH)_9NO_3$ (JCPDS: 791352). After being post-heated at 300 °C for 3 h, it began to transform to a new phase with much lower crystallinity. When the post-thermal treatment temperature was increased to 400 °C, the phase was totally converted into cubic Y_2O_3 phase, and the XRD pattern of the final product had no change except for the diffraction intensity as temperature was increased to 600 °C. Fig. 1(b) shows the XRD patterns of $Y_{1.85}M_{0.1}O_3$:0.05Eu^{3+} (M = Gd, Y, La, Zn, Li) prepared using the hydrothermal method after being post-heated at 600 °C for 3 h. All the XRD peaks were identified in terms of Y_2O_3 and no additional peak due to the introduction of M ions was found. When the lower valent cations enter into the Y_2O_3 lattice, such as Li^+ and Zn^{2+}, the charge can be compensated by oxygen vacancies, interstitial cation, etc. Due to the radius difference (r_{Li^+} = 0.76 À, $r_{Zn^{2+}}$ = 0.74 À, $r_{Y^{3+}}$ = 0.88 À) [22], it is difficult for Li^+ or Zn^{2+} to enter into interstitial sites of Y_2O_3, so it is assumed that the incorporated Li^+ or Zn^{2+} occupy the Y^{3+} sites and the extra charges are inclined to be compensated by oxygen vacancies.

Fig. 2 shows the TG/DTA results of $Y_{1.95}O_3$:0.05Eu^{3+} prepared using the hydrothermal method without thermal treatment. The precursor shows a two-step weight loss around 400 °C and 510 °C, and two endothermic peaks are located at the same temperature ranges, which indicates that (1) the as-synthesized precursor begins to convert to Y_2O_3 at 400 °C, and the conversion to Y_2O_3 is completed at 510 °C; and (2) Y_2O_3 was produced by a two-step decomposition of $Y_4O(OH)_9NO_3$ during the calcination process.

Fig. 3(a)–(b) show the typical TEM images of the obtained $Y_{1.95}O_3$:0.05Eu^{3+} particles, from which it can be seen that most of the samples obtained after being post-heated at 300 °C for 3 h display nano-rod morphologies, with diameters of 50–180 nm and lengths up to 800 nm, and the morphologies are still maintained except for the sizes even after thermal treatment at 600 °C for 3 h.